

DeepMoTion: Learning to Navigate Like Humans

Mahmoud Hamandi, Mike D’Arcy, and Pooyan Fazli¹

Abstract—We present a novel human-aware navigation approach, where the robot learns to mimic humans to navigate safely in crowds. The presented model referred to as DeepMoTion, is trained with pedestrian surveillance data to predict human velocity. The robot processes LiDAR scans via the trained network to navigate to the target location. We conduct extensive experiments to assess the different components of our network and prove the necessity of each to imitate humans. Our experiments show that DeepMoTion outperforms state-of-the-art in terms of human imitation and reaches the target on 100% of the test cases without breaching humans’ safe distance.

I. INTRODUCTION

Robots are gradually moving from factories and labs to streets, homes, offices, and healthcare facilities. These robots are currently assigned tasks that require interaction with humans, such as guiding passengers through busy airport terminals [1] or roaming around university buildings and interacting with nearby humans [2], [3].

As robots are increasingly becoming part of our everyday lives, it is essential for them to be aware of the surrounding humans while performing their tasks. Navigation is a basic skill for autonomous robots. We define human-aware navigation as the ability of the robot to navigate while complying with social norms and ensuring human safety.

While many existing systems allow robots to navigate safely within crowds [4], [5], they still rely heavily on manually-crafted models of human motion. Such models may capture the aspects of human motion as understood by their designers, while they may likely miss subtle trends that characterize their human aspect. In addition, manually-crafted models do not have a way to automatically adapt to different cultures, so it may require significant manual effort to be used in a different environment.

We present DeepMoTion (Deep Model for Target-driven Imitation), a deep imitation learning algorithm that eliminates the need for an explicit model of human motion and instead learns the human navigation patterns directly by observing pedestrians. Moreover, the network learns to decide on the direction and speed associated with raw LiDAR data without the need for any preprocessing or object classification. The network is trained to learn the possible motion patterns it might face in human crowds on its own.

The goal of this work is to learn directly from pedestrian data without the need for a predefined human model. With the absence of a true model, learning the reward governing human motion is not feasible with current Inverse Reinforcement Learning algorithms such as the one presented in [6].

Our method tackles the imitation problem as a classification one, where the network learns a specific command for each observation without simulating the learned policy. This approach reduces the amount of time required for each architecture test and allows us to explore multiple network configurations.

II. BACKGROUND AND STATE OF THE ART

Previous work on human-aware navigation suggested to apply hand-crafted models to control a robot about humans, define human-centric cost maps, or even follow humans through crowds.

Helbing and Molar [7] presented the Social Force Model (SFM), where they modeled the assumed social forces that govern the human motion. Ferrer *et al.* [4] used the social force model to navigate in a way similar to humans. In their work, the robot navigates to the target while abiding by the social forces, i.e. the robot is attracted by its target and repelled by pedestrians and obstacles. Furthermore, they extended the social force model to allow the robot to escort a human while providing a scheme to learn the parameters of the model.

Vasquez *et al.* [8] presented a human-aware navigation framework where they tested a variety of features such as crowd density and the social forces to learn a cost map that replicates the reward maximized in human navigation. To learn the cost map, they used a simulator with a built-in human model.

Bera *et al.* [9] predicted human motion after observing a set of related psychological cues such as aggressiveness, tension, and level of activity. The robot then deduces the acceptable path from the predicted human locations and social distances inferred from the same psychological features.

Another approach to human-aware navigation was presented by Mehta *et al.* [10], where the robot follows a human through crowds when it cannot navigate on its own. In their approach the robot decides to navigate freely when the scene is clear or compromise its optimal shortest path by following a human to its goal. When neither possibility is viable, the robot stops and waits for a clearance.

Sisbot *et al.* [5] suggested a set of human-centric costs that allow the robot to navigate safely about them. The method applied a cost-based navigational algorithm with a Gaussian coercing a safety distance about each human. In addition, the robot attempted to stay in the visual range of the existing pedestrians and to increase its own visibility near hidden areas, such as when rotating about a corner.

Lu and Smart [11] proposed another method where the robot navigates following a human-aware cost map. Their

¹ Mahmoud Hamandi, Mike D’Arcy, and Pooyan Fazli are with the Electrical Engineering and Computer Science Department, Cleveland State University, Cleveland, OH 44115, USA.

approach forces the robot to navigate on the right side of a hallway, allowing opposing humans to navigate on its left. In addition, the robot communicated its awareness of the nearby pedestrians by tilting its head toward their eyes.

While these methods provide a model for human motion, multiple deep learning architectures were also presented in the literature to learn any navigation algorithm. Pfeiffer *et al* [12] proposed an end-to-end network that allowed the robot to navigate based on LiDAR scans and target position. Similarly, Groshev *et al.* [13] presented a network that learns reactive policies that imitate a planning algorithm when provided with current and goal observations. Both papers presented novel ideas; however, they both learn reactive policies that ignore previous robot states while trying to imitate long term planning algorithms.

In conclusion, methods in the literature show the advantage of imitating humans, although they do not do so from actual human traces. In what follows, we intend to train directly from pedestrian data to alleviate the need for any human modeling through an end-to-end network.

III. PROBLEM DEFINITION

Figure 1 shows the different parts of our human imitation method. Our model is trained with the ETH pedestrian dataset [14] presenting videos of humans navigating in a real-world environment. The dataset contains environment maps and a set χ of humans, and for each human h the trajectory ζ_h that they took through the environment. Each ζ_h is a sequence of locations $l_{h,t}$, representing the position of human h at time t . We use a simulator to estimate LiDAR scans $\mathbf{z}_{h,t}$, velocities $\mathbf{v}_{h,t}$, and target locations $\tau_{h,t}$ for each human, which we then use to train the network to imitate the human trajectories. After training, the robot processes its target location and LiDAR scans via DeepMoTion to calculate navigational commands that allow it to reach the target safely while moving similarly to the humans in the dataset.

We contrast our human imitation problem with the literature on human trajectory prediction [15],[16] where the primary focus is predicting a human’s future position based on their current location, surroundings, and in some cases a history of previous states. The predictions in these methods are not conditioned on a known target, making them unsuitable for the navigation task, where we must be able to specify a destination for the robot to travel to. With human motion imitation, we assume the robot is given a target and its objective is to determine *how* a human would navigate to it. Therefore, the input to our method includes, in addition to the current state of the human, the direction of the target position.

IV. DEEPMOTION

DeepMoTion is a deep neural network $f(s_{h,t})$ defined as:

$$\begin{aligned} \{d_{h,t}, v_{h,t}\} &= f(s_{h,t}), \\ s_{h,t} &= [\mathbf{z}_{h,t-1}, \mathbf{z}_{h,t}, \tau_{h,t}]^T, \end{aligned} \quad (1)$$

where $s_{h,t}$ is the input state vector, and $\{d_{h,t}, v_{h,t}\}$ is the output action set describing the direction and magnitude of

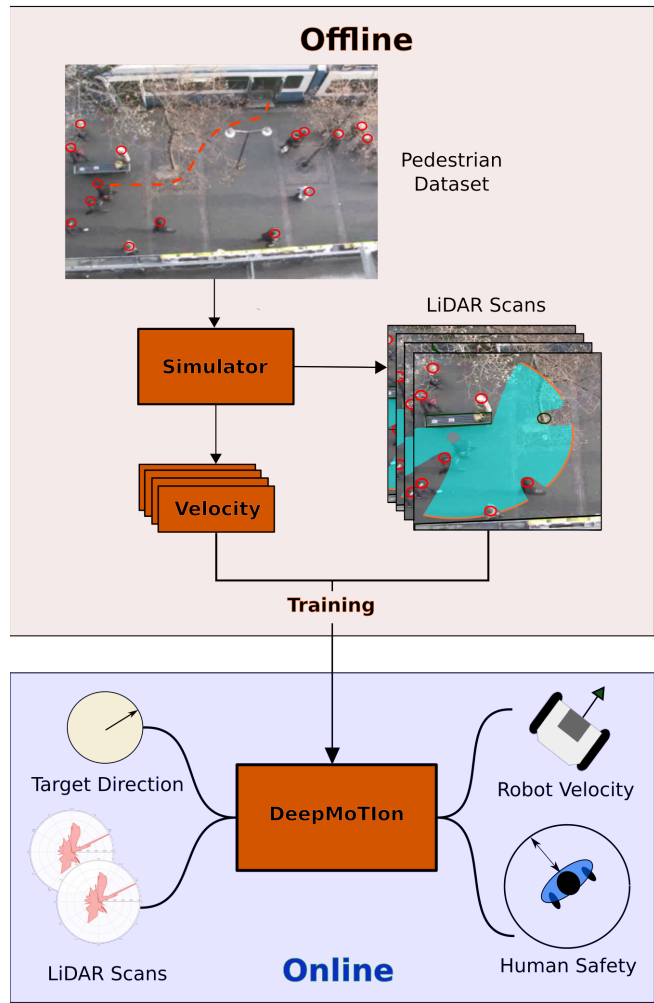


Fig. 1: Algorithm overview: human imitation learning with DeepMoTion.

the velocity $\mathbf{v}_{h,t}$. As shown in Equation (1), our network is trained to predict velocity commands to reach a target represented by its direction $\tau_{h,t}$, while processing the current and last raw LiDAR scans $\mathbf{z}_{h,(t-1,t)}$. The concatenation of the two LiDAR scans was necessary for the network to deduce static from dynamic obstacles and learn the motion pattern of the latter.

Our DNN architecture is shown in Figure 2. In this architecture the skip connections from the input were inspired by classical planning algorithms [13] such as value iteration and greedy search. However, after the convolutional layers we re-feed only the raw target direction to the network due to its direct correlation to the velocity direction, while the LiDAR scans add minimal value in their raw state. We found through experimentation that only shared convolutional layers were required for the network to correctly deduce the direction and speed from the input state while adding specialized convolutional layers for each of the two outputs reduced its performance.

In addition, for a planning algorithm each state and the

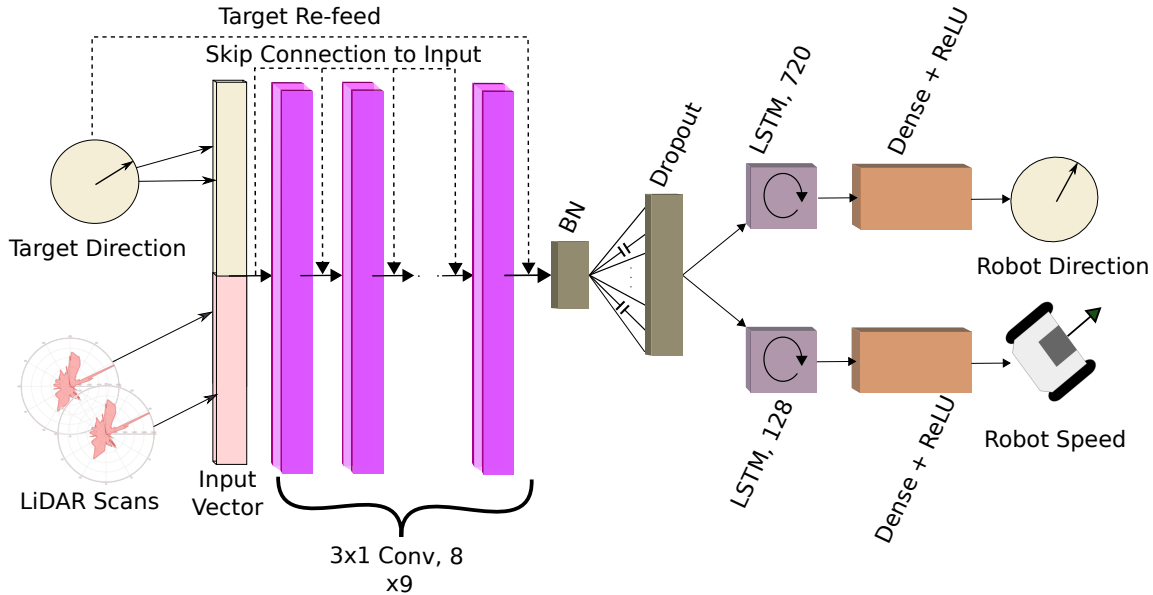


Fig. 2: DeepMoTion network architecture.

corresponding action are tightly related to the previous observations. The LSTM layer was added to the network to allow it to remember the past state of the environment, as these layers have been shown to improve the prediction of future states based on their memory of the past [17]. We later provide a thorough experimental comparison to show the LSTM’s necessity. Batch normalization was necessary to assure the boundedness of the input to the LSTM layers.

Finally, it should be noted that our algorithm runs in real-time despite the depth of the network due to the low dimensionality of its input state vector.

A. Loss Function

Our loss function is designed to train the network to output the direction and speed as seen in the human dataset by minimizing the squared error of the speed and the cross entropy error of the output direction.

However, human imitation presents a challenge due to their stochasticity. In fact, two humans might behave differently even with the same observations depending on their personality and other hidden factors. This suggests that the correct direction might be one of many directions in a range about the ground-truth. As such it is desirable to penalize the network less for cases where it is close to the ground truth than cases where it is completely wrong. To this end, we model the output direction as a Gaussian distribution about the human-chosen direction with a standard deviation σ as shown in Figure 3.

We also observe that humans closely approach obstacles and other humans. While this is acceptable between humans, a robot is typically less agile, so it must keep a larger distance to all obstacles to ensure the safety of both itself and humans. This motivates us to add a safety factor to the loss function that encourages a larger distance between the robot and the closest object around it.

As such, our complete loss function for a batch of N training examples can be expressed as follows:

$$\begin{aligned}
 & \underbrace{\frac{1}{N} \sum_{i=1}^N (v_i - \hat{v}_i)^2}_{\text{Speed Loss}} + \underbrace{\frac{1}{N} \sum_{i=1}^N H(d_i, \hat{d}_i(\sigma))}_{\text{Direction Loss}} \\
 & + \underbrace{\frac{1}{N} \sum_{i=1}^N \max(0, 1 - \log(\min(z_i) + 1 - \text{safeDistance}))}_{\text{Safety Loss}},
 \end{aligned} \tag{1}$$

where $H(p, q)$ is the cross entropy loss function, d_i is the predicted direction distribution, and $\hat{d}_i(\sigma)$ is the Gaussian distribution about the human-chosen direction with standard deviation σ .

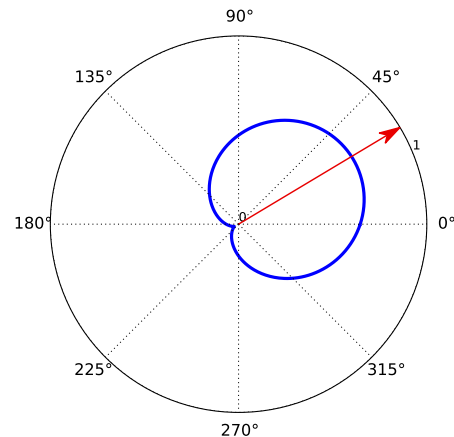


Fig. 3: Gaussian distribution (blue) about the human-chosen direction (red) with a standard deviation σ .

V. EXPERIMENTS

To evaluate the performance of DeepMoTion when imitating humans, we conducted experiments on the ETH BIWI walking pedestrians dataset [14]. The dataset provides annotated trajectories of 650 humans recorded over 25 minutes of time on two maps. To avoid overfitting and allow the network to generalize to unseen maps, the training data was augmented by replicating each path while rotating the map at random angles.

The dense crowds and sudden changes of pedestrian direction in this dataset make it sufficiently challenging for our experiments. We conducted two types of experiments on this dataset. First, we assessed the different components of the network, and then we benchmarked it against other human-aware and deep imitation learning methods to compare its safety and human-aware motion.

A. Benchmarks

To assess the performance of DeepMoTion, we compared our results with two deep learning algorithms as well as a human-aware navigation method from the literature.

- 1) **Generalized Reactive Planner (GRP)**: GRP is a deep neural network architecture composed of multiple convolutional layers, each with a skip connection from the input, followed by fully connected layers to the output [13]. In addition, the input of GRP is a concatenation of the observation and target. GRP is trained to learn reactive policies that allow the robot to imitate a planning algorithm.
- 2) **End-to-end Motion Planning (EMP)**: EMP is another deep neural network architecture that relies on a relatively small number of deep convolutional layers and two residual shortcut connections [12]. Moreover, the target in this network is provided after the convolutional layers. EMP is trained to learn a navigational algorithm.
- 3) **Social Force Model (SFM)**: SFM calculates a set of imaginary 'social' forces that govern human motion in a crowd [4]. These forces can be grouped as repulsive to obstacles and other humans as well as attractive to the target.

It should be noted that the comparison against SFM is symbolic in this work, as the objective of the presented algorithm is to navigate similarly to humans without hand-crafting a model of their motion. In addition, SFM requires the class of each object around it along with their locations. Such information requires processing of the raw sensor data, which was absent for the other algorithms.

B. Metrics

To assess our network and the benchmark algorithms, we compared their performance when trying to navigate from a start position to the final target. The start and final positions are chosen from the dataset, where the simulator replaces one of the humans with a robot and compares the resemblance of their paths, as well as the safety of the robot's. Formally, we

compare the performance of our network and the benchmark algorithms based on the following metrics:

- 1) **Squared Path Difference (SPD)**: The trajectories of the robot and the corresponding human are modeled as discrete-time trajectories $T_{r,0..n}$ and $T_{h,0..m}$ respectively. The squared path difference can then be expressed as

$$\sum_{i=1}^{\max(n,m)} \|T_{r,i} - T_{h,i}\|^2 \quad (2)$$
- 2) **Dynamic Time Warping (DTW)**: A path difference metric described in [18]. DTW finds the optimal time warp to match the segments of the two paths and measures the dissimilarity between them following that warp.
- 3) **Proximity**: Proximity is the closest distance the robot comes to a human on its path; in the case of any collision along the path, it is assigned a value of 0. We report the average proximity over all the test cases.
- 4) **Number of Collisions**: The number of times the robot collides with a human while navigating.
- 5) **Target**: The percentage of trials where the robot reached the goal within the 400-step threshold.

It should be noted that unlike most human-aware navigation papers [4],[19], we are reporting the average number of collisions as a comparison metric. However, when implemented in the real world, a low level obstacle avoidance controller is to be added to the algorithm to assure complete human safety and accommodate for any failures similar to [20].

C. Stochastic Output, Safety Loss, and DeepMoTion Variants

The necessity of the LSTM layer is shown by testing two variants of the network, where we refer to DeepMoTion_{LSTM} as the DNN with the architecture as explained before and DeepMoTion_{conv} as the DNN without any LSTM layers. More convolutional layers were added to DeepMoTion_{conv} to accommodate for the depth difference.

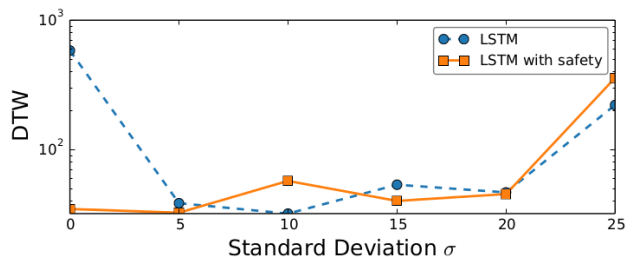


Fig. 4: Comparison of the path similarity metric *DTW* for the different variants of DeepMoTion_{LSTM} when varying σ .

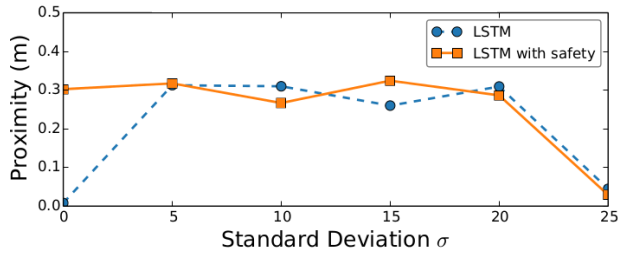


Fig. 5: Comparison of the safety metric (*proximity*) for the different variants of DeepMoTion_{LSTM} when varying σ .

Figure 4 shows the path difference metric *DTW*, and Figure 5 shows the average proximity of DeepMoTion while varying σ . DeepMoTion_{conv} was not shown in these figures due to the large difference in the corresponding metrics as compared with the LSTM variant; however, we provide a comparison of the metrics of the two networks in the next section. The figures show the benefit of the safety loss function for $\sigma = 0$, with DeepMoTion having a safer path and lower path difference when trained with the corresponding loss. The same figures show DeepMoTion_{LSTM} resilient to the safety loss for $\sigma > 0$ with small fluctuations due to random training noise. At $\sigma = 25$ we observe a decrease in performance of both networks, where the standard deviation is large enough that it induces more noise than it accommodates for the existing one. Ideally, the network should be trained with a variance equivalent to the training data in case it was present.

It appears that the safety loss and the standard deviation σ improve the imitation learning equally. This is observed in the values of *DTW* and proximity being the same for both networks at $\sigma > 0$, and these values being equivalent to the metrics of the network with safety loss at $\sigma = 0$. It is also observed from the two figures that the decrease in path difference is coupled with an increase in proximity. This suggests that the closer the robot’s path to the humans’ the safer its navigation, thus the advantage of imitating humans for navigation.

Figure 6 shows example robots navigating with the two variants of DeepMoTion’s architecture. Figure 6 (left) shows an example where DeepMoTion_{conv} is accumulating error throughout its path and finally misses the target; this behavior was observed throughout the trials on multiple occasions, which explains the difference in performance of the two networks. The figure also shows that DeepMoTion_{LSTM} was able to follow the human path all the way to the target. These observations suggest the necessity of the LSTM layer for the network to acknowledge the existence of the error and correct it when required. Figure 6 (right) shows an example where both networks reached the target, with the LSTM variant imitating the human closely.

D. Comparison with Benchmarks

Table I compares our network against the benchmark algorithms and assess each following the metrics presented in V-B.

TABLE I: Performance Metrics Comparison

	<i>SPD</i>	<i>DTW</i>	<i>Proximity</i>	<i>Collisions</i>	<i>Target</i>
DeepMoTion _{LSTM}	151	39	0.31	0.67	100%
DeepMoTion _{conv}	732	131	0.25	0.89	69%
SFM	3817	51	0.29	0.26	100%
EMP	15437	1187	0.001	7.69	32%
GRP	334	52	0.18	0.78	84%

Table I illustrates the ability of our network to imitate humans better than the other benchmarks for all the metrics, with the exception of SFM showing a lower rate of collision. *SPD* and *DTW* show that our network has the lowest path difference for all the tested algorithms, with the next best algorithm (GRP) showing more than double the path difference. While *SPD* reflects DeepMoTion’s ability to replicate both direction and speed, *DTW* compares the two paths irrespective of their velocities.

Table I also shows that DeepMoTion_{LSTM} reaches the target on 100% of the trials, while the other networks fail many with EMP reaching the target only 32% and GRP reaching the target 84% of the trials. The proximity parameter shows that our network keeps an average proximity of 0.31m to any human, while SFM keeps a 0.29m despite explicitly weighting its repulsive force to humans the most out of the other social forces. *Collisions* shows that SFM has the lowest number of collisions among all algorithms. This can be explained by the ability of the algorithms to stop in the case of dense crowds, while all the other networks were not trained on any human demonstration that exerted that type of behavior. We expect DeepMoTion to learn to stop and avoid collisions better when trained on more pedestrian data showing a wider set of possible navigation scenarios.

In addition, as discussed in the previous paragraph, the LSTM variant of DeepMoTion imitates humans much better than DeepMoTion_{conv}. This is shown in Table I, where DeepMoTion_{LSTM} exhibits a better performance for all metrics.

Finally, we note that our network was able to navigate even with a LiDAR range other than the one it was trained on. All the algorithms above were trained and tested on a LiDAR with a 30m range. To show the ability of our network to generalize to different ranges, we tested its performance with a LiDAR scanner with a 6m range without any retraining. The network was still able to reach the target on 97% of the trials, with an increase in *DTW* to 47, and a decrease in collisions to 0.51. The decrease in collisions was expected, as the network is observing obstacles in locations that were supposed to be free, and thus the robot becomes more careful.

VI. CONCLUSION AND FUTURE WORK

We introduced a novel deep imitation learning framework and studied its performance when learning to navigate from human traces. We trained the deep network to predict robot command velocities from raw LiDAR scans without the requirement of any preprocessing or classification of the surrounding objects. Our experiments showed DeepMoTion’s

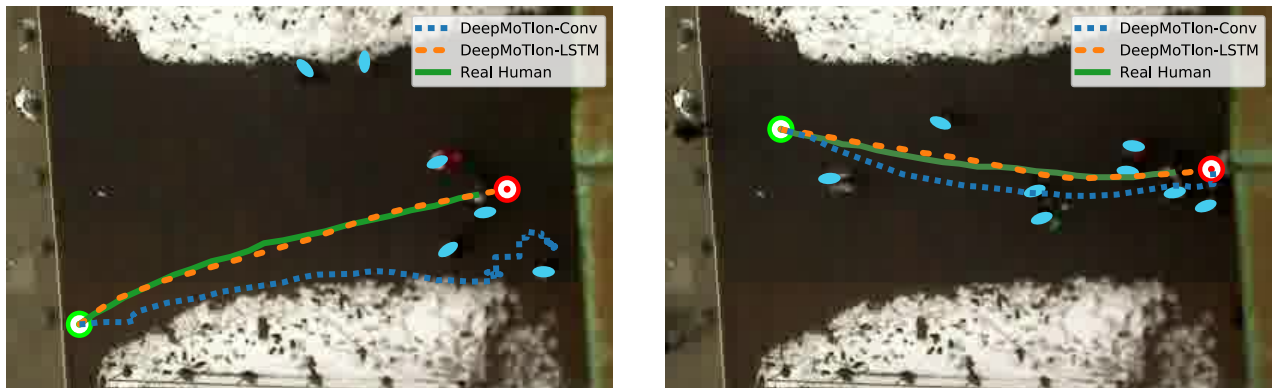


Fig. 6: Demonstrations of our network navigating from the start location (green) to the goal location (red). (left) shows a scenario where DeepMoTlon_{conv} fails, while DeepMoTlon_{LSTM} finds the target. (right) shows a case where both DeepMoTlon variants find the target avoiding humans.

ability to generate navigational commands similar to humans, and plan a path to the target on all test sets, outperforming all of the benchmarks on path difference metrics, and all except SFM on other metrics like collisions. In addition, we presented a comparative assessment that showed the necessity of an LSTM layer for a planning algorithm via a DNN, where the robot navigating with the non-LSTM variant of our network was led astray on many test cases. Finally, we presented a novel loss function to train the network. The loss function allowed us to accommodate for human motion stochasticity while at the same time forcing the robot to navigate safely.

In the future, we plan to train the network to navigate using raw images instead of LiDAR scans, where we believe the larger bandwidth of data can help the network understand human motion from their point of view. However, unlike DeepMoTlon , special consideration has to be taken when training the network with images to provide a navigation model that runs in real time when implemented on a mobile platform.

REFERENCES

- [1] R. Triebel, K. Arras, R. Alami, L. Beyer, S. Breuers, R. Chatila, M. Chetouani, D. Cremers, V. Evers, M. Fiore, *et al.*, “Spencer: A socially aware service robot for passenger guidance and help in busy airports,” in *Field and Service Robotics*. Springer, 2016, pp. 607–622.
- [2] M. Veloso, J. Biswas, B. Coltin, S. Rosenthal, T. Kollar, C. Mericli, M. Samadi, S. Brandao, and R. Ventura, “Cobots: Collaborative robots servicing multi-floor buildings,” in *Proceedings of the IEEE/RSJ International Conference on Intelligent Robots and Systems, IROS*, 2012, pp. 5446–5447.
- [3] U. Patel, E. Hatay, M. D’Arcy, G. Zand, and P. Fazli, “Beam: A collaborative autonomous mobile service robot,” in *Proceedings of the AAAI Fall Symposium on Artificial Intelligence for Human-Robot Interaction, AI-HRI 2017*, 2017.
- [4] G. Ferrer, A. G. Zulueta, F. H. Cotarelo, and A. Sanfeliu, “Robot social-aware navigation framework to accompany people walking side-by-side,” *Autonomous robots*, vol. 41, no. 4, pp. 775–793, 2017.
- [5] E. A. Sisbot, L. F. Marin-Urias, R. Alami, and T. Simeon, “A human aware mobile robot motion planner,” *IEEE Transactions on Robotics*, vol. 23, no. 5, pp. 874–883, 2007.
- [6] B. D. Ziebart, A. L. Maas, J. A. Bagnell, and A. K. Dey, “Maximum entropy inverse reinforcement learning,” in *Proceedings of the AAAI Conference on Artificial Intelligence, AAAI*, 2008, pp. 1433–1438.
- [7] D. Helbing and P. Molnar, “Social force model for pedestrian dynamics,” *Physical review E*, vol. 51, no. 5, p. 4282, 1995.
- [8] D. Vasquez, B. Okal, and K. O. Arras, “Inverse reinforcement learning algorithms and features for robot navigation in crowds: an experimental comparison,” in *Proceedings of the IEEE/RSJ International Conference on Intelligent Robots and Systems, IROS*, 2014, pp. 1341–1346.
- [9] A. Bera, T. Randhavane, R. Prinja, and D. Manocha, “Sociosense: Robot navigation amongst pedestrians with social and psychological constraints,” *arXiv preprint arXiv:1706.01102*, 2017.
- [10] D. Mehta, G. Ferrer, and E. Olson, “Autonomous navigation in dynamic social environments using multi-policy decision making,” in *Proceedings of the IEEE/RSJ International Conference on Intelligent Robots and Systems, IROS*, 2016, pp. 1190–1197.
- [11] D. V. Lu and W. D. Smart, “Towards more efficient navigation for robots and humans,” in *Proceedings of the IEEE/RSJ International Conference On Intelligent Robots and Systems, IROS*, 2013, pp. 1707–1713.
- [12] M. Pfeiffer, M. Schaeuble, J. Nieto, R. Siegwart, and C. Cadena, “From perception to decision: A data-driven approach to end-to-end motion planning for autonomous ground robots,” in *Proceedings of the IEEE International Conference on Robotics and Automation, ICRA*, 2017, pp. 1527–1533.
- [13] E. Groshev, A. Tamar, S. Srivastava, and P. Abbeel, “Learning generalized reactive policies using deep neural networks,” *arXiv preprint arXiv:1708.07280*, 2017.
- [14] S. Pellegrini, A. Ess, K. Schindler, and L. Van Gool, “You’ll never walk alone: Modeling social behavior for multi-target tracking,” in *Proceedings of the 12th IEEE International Conference on Computer Vision, ICCV*, 2009, pp. 261–268.
- [15] A. Alahi, K. Goel, V. Ramanathan, A. Robicquet, L. Fei-Fei, and S. Savarese, “Social lstm: Human trajectory prediction in crowded spaces,” in *Proceedings of the IEEE Conference on Computer Vision and Pattern Recognition, CVPR*, 2016, pp. 961–971.
- [16] T. Fernando, S. Denman, S. Sridharan, and C. Fookes, “Soft+ hard-wired attention: An lstm framework for human trajectory prediction and abnormal event detection,” *arXiv preprint arXiv:1702.05552*, 2017.
- [17] K. Greff, R. K. Srivastava, J. Koutník, B. R. Steunebrink, and J. Schmidhuber, “Lstm: A search space odyssey,” *IEEE Transactions on Neural Networks and Learning Systems*, vol. 28, no. 10, pp. 2222–2232, 2017.
- [18] J. B. KRUSKALL, “The symmetric time-warping problem : From continuous to discrete,” *Time Warps, String Edits, and Macromolecules : The Theory and Practice of Sequence Comparison*, pp. 125–161, 1983. [Online]. Available: <https://ci.nii.ac.jp/naid/10011461178/en/>
- [19] D. Vasquez, P. Stein, J. Rios-Martinez, A. Escobedo, A. Spalanzani, and C. Laugier, “Human aware navigation for assistive robotics,” in *Experimental Robotics*. Springer, 2013, pp. 449–462.
- [20] B. Kim and J. Pineau, “Socially adaptive path planning in human environments using inverse reinforcement learning,” *International Journal of Social Robotics*, vol. 8, no. 1, pp. 51–66, 2016.